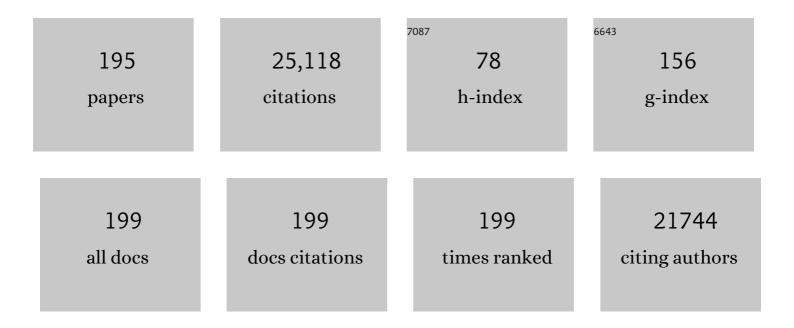
## **Yet-Ming Chiang**

List of Publications by Year in descending order

Source: https://exaly.com/author-pdf/2794014/publications.pdf Version: 2024-02-01



#	Article	IF	CITATIONS
1	A generalized reduced fluid dynamic model for flow fields and electrodes in redox flow batteries. AICHE Journal, 2022, 68, .	1.8	6
2	Exploring the Synthesis of Alkali Metal Anti-perovskites. Chemistry of Materials, 2022, 34, 947-958.	3.2	13
3	The challenges and opportunities of battery-powered flight. Nature, 2022, 601, 519-525.	13.7	143
4	The iron-energy nexus: A new paradigm for long-duration energy storage at scale and clean steelmaking. One Earth, 2022, 5, 212-215.	3.6	4
5	A Comparative Study of Compressive Effects on the Morphology and Performance of Carbon Paper and Cloth Electrodes in Redox Flow Batteries. Energy Technology, 2022, 10, .	1.8	7
6	State of LiFePO <sub>4</sub> Li-Ion Battery Electrodes after 6533 Deep-Discharge Cycles Characterized by Combined Micro-XRF and Micro-XRD. ACS Applied Energy Materials, 2022, 5, 4358-4368.	2.5	2
7	Electrochemical Stability and Reversibility of Aqueous Polysulfide Electrodes Cycled Beyond the Solubility Limit. Journal of the Electrochemical Society, 2022, 169, 060524.	1.3	1
8	Microstructural engineering of high-power redox flow battery electrodes via non-solvent induced phase separation. Cell Reports Physical Science, 2022, 3, 100943.	2.8	13
9	Semi-solid alkali metal electrodes enabling high critical current densities in solid electrolyte batteries. Nature Energy, 2021, 6, 314-322.	19.8	78
10	Nonâ€5olvent Induced Phase Separation Enables Designer Redox Flow Battery Electrodes. Advanced Materials, 2021, 33, e2006716.	11.1	35
11	Redox Flow Batteries: Nonâ€Solvent Induced Phase Separation Enables Designer Redox Flow Battery Electrodes (Adv. Mater. 16/2021). Advanced Materials, 2021, 33, 2170126.	11.1	0
12	An Operando calorimeter for high temperature electrochemical cells. JPhys Energy, 2021, 3, 034007.	2.3	0
13	Leveraging Neural Networks and Genetic Algorithms to Refine Electrode Properties in Redox Flow Batteries. Journal of the Electrochemical Society, 2021, 168, 050547.	1.3	5
14	Enabling High-Rate Plating in Solid-State Li Batteries By Interface Engineering and Pulse Plating. ECS Meeting Abstracts, 2021, MA2021-01, 434-434.	0.0	0
15	Electrochemical Residence Time Distribution As a Diagnostic Tool for Electrodes in Redox Flow Batteries. ECS Meeting Abstracts, 2021, MA2021-01, 974-974.	0.0	0
16	Analytical and Numerical Modeling of Microelectrode Voltammetry in Oblate Spheroidal Coordinates. ECS Meeting Abstracts, 2021, MA2021-01, 1803-1803.	0.0	0
17	(Energy Technology Division Graduate Student Award sponsored by Bio-Logic) Designer Porous Carbon Electrodes for Redox Flow Batteries. ECS Meeting Abstracts, 2021, MA2021-01, 240-240.	0.0	0
18	(Student Battery Slam Best Presentation Award Winner) Combining Experimentation and Computation for Accelerated Understanding of Electrode Morphology in Redox Flow Batteries. ECS Meeting Abstracts, 2021, MA2021-01, 266-266.	0.0	0

#	Article	IF	CITATIONS
19	A Flow-through Microelectrode Sensor for Monitoring in Operando Concentrations in Redox Flow Batteries. ECS Meeting Abstracts, 2021, MA2021-01, 218-218.	0.0	0
20	Establishing a unified framework for ion solvation and transport in liquid and solid electrolytes. Trends in Chemistry, 2021, 3, 807-818.	4.4	27
21	Non-Arrhenius Ionic Conductivity Transitions in Sodium Antiperovskite Ionic Conductors. ECS Meeting Abstracts, 2021, MA2021-02, 43-43.	0.0	2
22	Temperature Dependent Anion Rotational Dynamics Correlated to Cation Transport in Cluster Ion Anti-Perovskites. ECS Meeting Abstracts, 2021, MA2021-02, 1-1.	0.0	0
23	Limited Accessibility to Surface Area Generated by Thermal Pretreatment of Electrodes Reduces Its Impact on Redox Flow Battery Performance. ACS Applied Energy Materials, 2021, 4, 13516-13527.	2.5	11
24	Microelectrode-Based Sensor for Measuring <i>Operando</i> Active Species Concentrations in Redox Flow Cells. ACS Applied Energy Materials, 2021, 4, 13830-13840.	2.5	11
25	(Invited) Semi-Solid Alkali Metal Electrodes Enabling High Critical Current Densities and Accessible Areal Capacities in Solid Electrolyte Batteries. ECS Meeting Abstracts, 2021, MA2021-02, 335-335.	0.0	0
26	(Invited) Designing Fault-Tolerant Interfaces Between Metal Electrodes and Solid Electrolytes. ECS Meeting Abstracts, 2021, MA2021-02, 233-233.	0.0	0
27	Toward electrochemical synthesis of cement—An electrolyzer-based process for decarbonating CaCO <sub>3</sub> while producing useful gas streams. Proceedings of the National Academy of Sciences of the United States of America, 2020, 117, 12584-12591.	3.3	109
28	Design principles for self-forming interfaces enabling stable lithium-metal anodes. Proceedings of the National Academy of Sciences of the United States of America, 2020, 117, 27195-27203.	3.3	44
29	Data-driven electrode parameter identification for vanadium redox flow batteries through experimental and numerical methods. Applied Energy, 2020, 279, 115530.	5.1	26
30	Modelling of redox flow battery electrode processes at a range of length scales: a review. Sustainable Energy and Fuels, 2020, 4, 5433-5468.	2.5	29
31	Dynamics of Hydroxyl Anions Promotes Lithium Ion Conduction in Antiperovskite Li <sub>2</sub> OHCl. Chemistry of Materials, 2020, 32, 8481-8491.	3.2	53
32	Ultrathin Conformal oCVD PEDOT Coatings on Carbon Electrodes Enable Improved Performance of Redox Flow Batteries. Advanced Materials Interfaces, 2020, 7, 2000855.	1.9	22
33	Energy storage emerging: A perspective from the Joint Center for Energy Storage Research. Proceedings of the National Academy of Sciences of the United States of America, 2020, 117, 12550-12557.	3.3	218
34	Ultrafast ion transport at a cathode–electrolyte interface and its strong dependence on salt solvation. Nature Energy, 2020, 5, 578-586.	19.8	104
35	Exploration of Biomass-Derived Activated Carbons for Use in Vanadium Redox Flow Batteries. ACS Sustainable Chemistry and Engineering, 2020, 8, 9472-9482.	3.2	33
36	Comparing Physical and Electrochemical Properties of Different Weave Patterns for Carbon Cloth Electrodes in Redox Flow Batteries. Journal of Electrochemical Energy Conversion and Storage, 2020, 17, .	1.1	35

#	Article	IF	CITATIONS
37	Effect of Concentrated Diglyme-Based Electrolytes on the Electrochemical Performance of Potassium-Ion Batteries. ACS Applied Energy Materials, 2019, 2, 6051-6059.	2.5	44
38	Design Rules for Membranes from Polymers of Intrinsic Microporosity for Crossover-free Aqueous Electrochemical Devices. Joule, 2019, 3, 2968-2985.	11.7	84
39	Reducing Transformation Strains during Na Intercalation in Olivine FePO <sub>4</sub> Cathodes by Mn Substitution. ACS Applied Energy Materials, 2019, 2, 8060-8067.	2.5	15
40	Storage Requirements and Costs of Shaping Renewable Energy Toward Grid Decarbonization. Joule, 2019, 3, 2134-2153.	11.7	251
41	Electrochemical Redox Behavior of Li Ion Conducting Sulfide Solid Electrolytes. Chemistry of Materials, 2019, 31, 707-713.	3.2	94
42	Learning only buys you so much: Practical limits on battery price reduction. Applied Energy, 2019, 239, 218-224.	5.1	115
43	Producing High Concentrations of Hydrogen in Palladium via Electrochemical Insertion from Aqueous and Solid Electrolytes. Chemistry of Materials, 2019, 31, 4234-4245.	3.2	32
44	Revisiting the cold case of cold fusion. Nature, 2019, 570, 45-51.	13.7	48
45	Order–disorder transition in nano-rutile TiO <sub>2</sub> anodes: a high capacity low-volume change Li-ion battery material. Nanoscale, 2019, 11, 12347-12357.	2.8	40
46	Apparatus for <i> <b>operando</b> </i> x-ray diffraction of fuel electrodes in high temperature solid oxide electrochemical cells. Review of Scientific Instruments, 2019, 90, 023910.	0.6	6
47	Demonstrating Near-Carbon-Free Electricity Generation from Renewables and Storage. Joule, 2019, 3, 2585-2588.	11.7	21
48	Fabrication of Lowâ€Tortuosity Ultrahighâ€Areaâ€Capacity Battery Electrodes through Magnetic Alignment of Emulsionâ€Based Slurries. Advanced Energy Materials, 2019, 9, 1802472.	10.2	100
49	Stabilizing Li–S Battery Through Multilayer Encapsulation of Sulfur. Advanced Energy Materials, 2019, 9, 1802213.	10.2	66
50	Battery Electrodes: Fabrication of Low-Tortuosity Ultrahigh-Area-Capacity Battery Electrodes through Magnetic Alignment of Emulsion-Based Slurries (Adv. Energy Mater. 2/2019). Advanced Energy Materials, 2019, 9, 1970006.	10.2	2
51	Phase-field model for diffusion-induced grain boundary migration: An application to battery electrodes. Physical Review Materials, 2019, 3, .	0.9	10
52	Impact of Pore Tortuosity on Electrode Kinetics in Lithium Battery Electrodes: Study in Directionally Freeze-Cast LiNi <sub>0.8</sub> Co <sub>0.15</sub> Al <sub>0.05</sub> O <sub>2</sub> (NCA). Journal of the Electrochemical Society, 2018, 165, A388-A395.	1.3	97
53	Single-particle measurements of electrochemical kinetics in NMC and NCA cathodes for Li-ion batteries. Energy and Environmental Science, 2018, 11, 860-871.	15.6	224
54	Lithium Metal Penetration Induced by Electrodeposition through Solid Electrolytes: Example in Single-Crystal Li <sub>6</sub> La <sub>3</sub> ZrTaO <sub>12</sub> Garnet. Journal of the Electrochemical Society, 2018, 165, A3648-A3655.	1.3	172

#	Article	IF	CITATIONS
55	Enhancing the Performance of Viscous Electrode-Based Flow Batteries Using Lubricant-Impregnated Surfaces. ACS Applied Energy Materials, 2018, 1, 3614-3621.	2.5	8
56	Net-zero emissions energy systems. Science, 2018, 360, .	6.0	1,165
57	Structure, Chemistry, and Charge Transfer Resistance of the Interface between Li <sub>7</sub> La <sub>3</sub> Zr <sub>2</sub> O <sub>12</sub> Electrolyte and LiCoO <sub>2</sub> Cathode. Chemistry of Materials, 2018, 30, 6259-6276.	3.2	125
58	3D printing metals like thermoplastics: Fused filament fabrication of metallic glasses. Materials Today, 2018, 21, 697-702.	8.3	119
59	Electrochemical Characterization of High Energy Density Graphite Electrodes Made by Freeze-Casting. ACS Applied Energy Materials, 2018, 1, 4976-4981.	2.5	58
60	Electrochemomechanical Fatigue: Decoupling Mechanisms of Fracture-Induced Performance Degradation in Li <sub>X</sub> Mn <sub>2</sub> O <sub>4</sub> . Journal of the Electrochemical Society, 2018, 165, A2458-A2466.	1.3	22
61	Mesoscopic Phase Transition Kinetics in Secondary Particles of Electrode-Active Materials in Lithium-Ion Batteries. Chemistry of Materials, 2018, 30, 4216-4225.	3.2	18
62	Mechanical instability of electrode-electrolyte interfaces in solid-state batteries. Physical Review Materials, 2018, 2, .	0.9	69
63	Compliant Yet Brittle Mechanical Behavior of Li <sub>2</sub> S–P <sub>2</sub> S <sub>5</sub> Lithiumâ€lonâ€Conducting Solid Electrolyte. Advanced Energy Materials, 2017, 7, 1602011.	10.2	219
64	Accommodating High Transformation Strains in Battery Electrodes via the Formation of Nanoscale Intermediate Phases: Operando Investigation of Olivine NaFePO <sub>4</sub> . Nano Letters, 2017, 17, 1696-1702.	4.5	49
65	The Effect of Stress on Battery-Electrode Capacity. Journal of the Electrochemical Society, 2017, 164, A645-A654.	1.3	109
66	Electrodeposition Kinetics in Li-S Batteries: Effects of Low Electrolyte/Sulfur Ratios and Deposition Surface Composition. Journal of the Electrochemical Society, 2017, 164, A917-A922.	1.3	159
67	Effect of transition metal substitution on elastoplastic properties of LiMn2O4 spinel. Journal of Electroceramics, 2017, 38, 215-221.	0.8	8
68	Review—Practical Challenges Hindering the Development of Solid State Li Ion Batteries. Journal of the Electrochemical Society, 2017, 164, A1731-A1744.	1.3	536
69	Two-dimensional lithium diffusion behavior and probable hybrid phase transformation kinetics in olivine lithium iron phosphate. Nature Communications, 2017, 8, 1194.	5.8	85
70	Random Walk Analysis of the Effect of Mechanical Degradation on All-Solid-State Battery Power. Journal of the Electrochemical Society, 2017, 164, A2660-A2664.	1.3	19
71	Air-Breathing Aqueous Sulfur Flow Battery for Ultralow-Cost Long-Duration Electrical Storage. Joule, 2017, 1, 306-327.	11.7	151
72	Lowering the Bar on Battery Cost. Joule, 2017, 1, 212-219.	11.7	11

#	Article	IF	CITATIONS
73	Modeling of internal mechanical failure of all-solid-state batteries during electrochemical cycling, and implications for battery design. Journal of Materials Chemistry A, 2017, 5, 19422-19430.	5.2	191
74	Low-profile self-sealing sample transfer flexure box. Review of Scientific Instruments, 2017, 88, 083705.	0.6	4
75	Mechanism of Lithium Metal Penetration through Inorganic Solid Electrolytes. Advanced Energy Materials, 2017, 7, 1701003.	10.2	780
76	Connecting Particle Fracture with Electrochemical Impedance in Li <sub>X</sub> Mn <sub>2</sub> O <sub>4</sub> . Journal of the Electrochemical Society, 2017, 164, A3709-A3717.	1.3	18
77	Molecular understanding of polyelectrolyte binders that actively regulate ion transport in sulfur cathodes. Nature Communications, 2017, 8, 2277.	5.8	117
78	Solvent Effects on Polysulfide Redox Kinetics and Ionic Conductivity in Lithium-Sulfur Batteries. Journal of the Electrochemical Society, 2016, 163, A3111-A3116.	1.3	74
79	A low-dissipation, pumpless, gravity-induced flow battery. Energy and Environmental Science, 2016, 9, 1760-1770.	15.6	39
80	Characterization of Electronic and Ionic Transport in Li <sub>1-</sub> <i><sub>x</sub></i> Ni <sub>0.33</sub> Mn <sub>0.33</sub> Co <sub>0.33</sub> O <sub>2and Li<sub>1-</sub><i><sub>x</sub></i>Ni<sub>0.50</sub>Mn<sub>0.20</sub>Co<sub>0.30</sub>O<sub>22</sub></sub>	1.3	201
81	as a Function of Li Content. Journal of the Electrochemical Society, 2016, 163, A1512-A1517. Formulation of the coupled electrochemical–mechanical boundary-value problem, with applications to transport of multiple charged species. Acta Materialia, 2016, 104, 33-51.	3.8	44
82	Engineering the Transformation Strain in LiMn <sub><i>y</i></sub> Fe <sub>1–<i>y</i></sub> PO <sub>4</sub> Olivines for Ultrahigh Rate Battery Cathodes. Nano Letters, 2016, 16, 2375-2380.	4.5	45
83	Identification of Li-Ion Battery SEI Compounds through <sup>7</sup> Li and <sup>13</sup> C Solid-State MAS NMR Spectroscopy and MALDI-TOF Mass Spectrometry. ACS Applied Materials & Interfaces, 2016, 8, 371-380.	4.0	49
84	Three-Dimensional Growth of Li <sub>2</sub> S in Lithium–Sulfur Batteries Promoted by a Redox Mediator. Nano Letters, 2016, 16, 549-554.	4.5	199
85	Colloidal Suspensions: Biphasic Electrode Suspensions for Li-Ion Semi-solid Flow Cells with High Energy Density, Fast Charge Transport, and Low-Dissipation Flow (Adv. Energy Mater. 15/2015). Advanced Energy Materials, 2015, 5, n/a-n/a.	10.2	0
86	Mechanism and Kinetics of Li <sub>2</sub> S Precipitation in Lithium–Sulfur Batteries. Advanced Materials, 2015, 27, 5203-5209.	11.1	704
87	Biphasic Electrode Suspensions for Liâ€Ion Semiâ€solid Flow Cells with High Energy Density, Fast Charge Transport, and Lowâ€Dissipation Flow. Advanced Energy Materials, 2015, 5, 1500535.	10.2	76
88	XANES Investigation of Dynamic Phase Transition in Olivine Cathode for Liâ€ <del>l</del> on Batteries. Advanced Energy Materials, 2015, 5, 1500663.	10.2	22
89	Mitigating mechanical failure of crystalline silicon electrodes for lithium batteries by morphological design. Physical Chemistry Chemical Physics, 2015, 17, 17718-17728.	1.3	25
90	Phase Transitions: XANES Investigation of Dynamic Phase Transition in Olivine Cathode for Li-Ion Batteries (Adv. Energy Mater. 15/2015). Advanced Energy Materials, 2015, 5, n/a-n/a.	10.2	1

#	Article	IF	CITATIONS
91	Component-cost and performance based comparison of flow and static batteries. Journal of Power Sources, 2015, 293, 1032-1038.	4.0	12
92	The synergetic effect of lithium polysulfide and lithium nitrate to prevent lithium dendrite growth. Nature Communications, 2015, 6, 7436.	5.8	1,250
93	Improving the Capacity of Sodium Ion Battery Using a Virus-Templated Nanostructured Composite Cathode. Nano Letters, 2015, 15, 2917-2921.	4.5	70
94	Characterization of Electronic and Ionic Transport in Li <sub>1-</sub> <i><sub>x</sub></i> Ni <sub>0</sub> <i><sub>.</sub></i> Sub>Co <sub>0.15</sub> A Journal of the Electrochemical Society, 2015, 162, A1163-A1169.	l≺suub≫0.0	5 <b 90b>O <su< td=""></su<>
95	Supramolecular Perylene Bisimide-Polysulfide Gel Networks as Nanostructured Redox Mediators in Dissolved Polysulfide Lithium–Sulfur Batteries. Chemistry of Materials, 2015, 27, 6765-6770.	3.2	78
96	Electrochemical Charge Transfer Reaction Kinetics at the Silicon-Liquid Electrolyte Interface. Journal of the Electrochemical Society, 2015, 162, A7129-A7134.	1.3	49
97	Reversible Aluminumâ€lon Intercalation in Prussian Blue Analogs and Demonstration of a Highâ€Power Aluminumâ€lon Asymmetric Capacitor. Advanced Energy Materials, 2015, 5, 1401410.	10.2	142
98	Strategies to Avert Electrochemical Shock and Their Demonstration in Spinels. Journal of the Electrochemical Society, 2014, 161, F3005-F3009.	1.3	17
99	In Situ Observation of Random Solid Solution Zone in LiFePO <sub>4</sub> Electrode. Nano Letters, 2014, 14, 4005-4010.	4.5	104
100	Na3Ti2(PO4)3 as a sodium-bearing anode for rechargeable aqueous sodium-ion batteries. Electrochemistry Communications, 2014, 44, 12-15.	2.3	63
101	Polysulfide Flow Batteries Enabled by Percolating Nanoscale Conductor Networks. Nano Letters, 2014, 14, 2210-2218.	4.5	201
102	Maximizing Energetic Efficiency in Flow Batteries Utilizing Non-Newtonian Fluids. Journal of the Electrochemical Society, 2014, 161, A486-A496.	1.3	83
103	Effect of Electrochemical Charging on Elastoplastic Properties and Fracture Toughness of Li <sub>X</sub> CoO <sub>2</sub> . Journal of the Electrochemical Society, 2014, 161, F3084-F3090.	1.3	68
104	Electroactive-Zone Extension in Flow-Battery Stacks. Electrochimica Acta, 2014, 147, 460-469.	2.6	34
105	Quantifying reliability statistics for electrochemical shock of brittle materials. Journal of the Mechanics and Physics of Solids, 2014, 70, 71-83.	2.3	4
106	Design of Battery Electrodes with Dualâ€Scale Porosity to Minimize Tortuosity and Maximize Performance. Advanced Materials, 2013, 25, 1254-1258.	11.1	252
107	Aqueous semi-solid flow cell: demonstration and analysis. Physical Chemistry Chemical Physics, 2013, 15, 15833.	1.3	112
108	Electrochemical Shock in Ion-Intercalation Materials with Limited Solid-Solubility. Journal of the Electrochemical Society, 2013, 160, A1286-A1292.	1.3	52

#	Article	IF	CITATIONS
109	Electronic Conductivity in the Li <sub>4/3</sub> Ti <sub>5/3</sub> O <sub>4</sub> –Li <sub>7/3</sub> Ti <sub>5/3</sub> O <sub>4</sub> System and Variation with Stateâ€ofâ€Charge as a Li Battery Anode. Advanced Energy Materials, 2013, 3, 1125-1129.	10.2	90
110	Towards High Power High Energy Aqueous Sodiumâ€ion Batteries: The NaTi <sub>2</sub> (PO <sub>4</sub> ) <sub>3</sub> /Na <sub>0.44</sub> MnO <sub>2</sub> System. Advanced Energy Materials, 2013, 3, 290-294.	10.2	430
111	An Analytical Method to Determine Tortuosity in Rechargeable Battery Electrodes. Journal of the Electrochemical Society, 2012, 159, A548-A552.	1.3	112
112	Design criteria for electrochemical shock resistant battery electrodes. Energy and Environmental Science, 2012, 5, 8014.	15.6	146
113	Nanomechanical Quantification of Elastic, Plastic, and Fracture Properties of LiCoO <sub>2</sub> . Advanced Energy Materials, 2012, 2, 940-944.	10.2	74
114	Modeling the hydrodynamic and electrochemical efficiency of semi-solid flow batteries. Electrochimica Acta, 2012, 69, 301-307.	2.6	73
115	Semiâ€Solid Lithium Rechargeable Flow Battery. Advanced Energy Materials, 2011, 1, 511-516.	10.2	482
116	Templated self-assembly of non-close-packed colloidal crystals: Toward diamond cubic and novel heterostructures. Journal of Materials Research, 2011, 26, 247-253.	1.2	8
117	Reply to Comment on "Aliovalent Substitutions in Olivine Lithium Iron Phosphate and Impact on Structure and Propertiesâ€: Advanced Functional Materials, 2010, 20, 189-191.	7.8	18
118	Ultrahighâ€Energyâ€Density Microbatteries Enabled by New Electrode Architecture and Micropackaging Design. Advanced Materials, 2010, 22, E139-44.	11.1	156
119	Modeling the competing phase transition pathways in nanoscale olivine electrodes. Electrochimica Acta, 2010, 56, 969-976.	2.6	43
120	Electronically conductive phospho-olivines as lithium storage electrodes. , 2010, , 205-210.		2
121	"Electrochemical Shock―of Intercalation Electrodes: A Fracture Mechanics Analysis. Journal of the Electrochemical Society, 2010, 157, A1052.	1.3	274
122	Long range interactions in nanoscale science. Reviews of Modern Physics, 2010, 82, 1887-1944.	16.4	359
123	Electrochemically Driven Phase Transitions in Insertion Electrodes for Lithium-Ion Batteries: Examples in Lithium Metal Phosphate Olivines. Annual Review of Materials Research, 2010, 40, 501-529.	4.3	151
124	Properties of lithium phosphorus oxynitride (Lipon) for 3D solid-state lithium batteries. Journal of Materials Research, 2010, 25, 1507-1515.	1.2	39
125	Comparative Study of Lithium Transport Kinetics in Olivine Cathodes for Li-ion Batteries. Chemistry of Materials, 2010, 22, 1088-1097.	3.2	79
126	Building a Better Battery. Science, 2010, 330, 1485-1486.	6.0	413

#	Article	IF	CITATIONS
127	Overpotential-Dependent Phase Transformation Pathways in Lithium Iron Phosphate Battery Electrodes. Chemistry of Materials, 2010, 22, 5845-5855.	3.2	109
128	Aliovalent Substitutions in Olivine Lithium Iron Phosphate and Impact on Structure and Properties. Advanced Functional Materials, 2009, 19, 1060-1070.	7.8	265
129	Anisotropic wetting of ZnO by Bi2O3 with and without nanometer-thick surficial amorphous films. Acta Materialia, 2008, 56, 862-873.	3.8	28
130	Wetting and Prewetting on Ceramic Surfaces. Annual Review of Materials Research, 2008, 38, 227-249.	4.3	115
131	Electrochemically Induced Phase Transformation in Nanoscale Olivines Li <sub>1â~'<i>x</i></sub> MPO <sub>4</sub> (M = Fe, Mn). Chemistry of Materials, 2008, 20, 6189-6198.	3.2	121
132	Stamped microbattery electrodes based on self-assembled M13 viruses. Proceedings of the National Academy of Sciences of the United States of America, 2008, 105, 17227-17231.	3.3	144
133	Nanometer-Scale Wetting of the Silicon Surface by Its Equilibrium Oxide. Langmuir, 2008, 24, 1891-1896.	1.6	7
134	Modeling Particle Size Effects on Phase Stability and Transition Pathways in Nanosized Olivine Cathode Particles. Materials Research Society Symposia Proceedings, 2008, 1100, 3041.	0.1	2
135	Spatially Resolved Modeling of Microstructurally Complex Battery Architectures. Journal of the Electrochemical Society, 2007, 154, A856.	1.3	81
136	Size-Dependent Lithium Miscibility Gap in Nanoscale Li[sub 1â^'x]FePO[sub 4]. Electrochemical and Solid-State Letters, 2007, 10, A134.	2.2	413
137	Assembly of Metal Nanoparticles into Nanogaps. Small, 2007, 3, 488-499.	5.2	114
138	Pressure-balance and diffuse-interface models for surficial amorphous films. Materials Science & Engineering A: Structural Materials: Properties, Microstructure and Processing, 2006, 422, 19-28.	2.6	41
139	Virus-Enabled Synthesis and Assembly of Nanowires for Lithium Ion Battery Electrodes. Science, 2006, 312, 885-888.	6.0	1,756
140	Nanometer-Thick Surficial Films in Oxides as a Case of Prewetting. Langmuir, 2005, 21, 7358-7365.	1.6	62
141	Microstructural Modeling and Design of Rechargeable Lithium-Ion Batteries. Journal of the Electrochemical Society, 2005, 152, A255.	1.3	269
142	Comparative studies of the electronic structure of LiFePO4, FePO4, Li3PO4, LiMnPO4, LiCoPO4, and LiNiPO4. Journal of Applied Physics, 2004, 95, 6583-6585.	1.1	58
143	Electronic Structure and Electrical Conductivity of Undoped LiFePO[sub 4]. Electrochemical and Solid-State Letters, 2004, 7, A131.	2.2	131
144	On the electronic conductivity of phospho-olivines as lithium storage electrodes. Nature Materials, 2003, 2, 702-703.	13.3	52

#	Article	IF	CITATIONS
145	Peptides with selective affinity for carbon nanotubes. Nature Materials, 2003, 2, 196-200.	13.3	520
146	Electrochemically-driven solid-state amorphization in lithium–metal anodes. Journal of Power Sources, 2003, 119-121, 604-609.	4.0	177
147	Electrochemically-driven solid-state amorphization in lithium-silicon alloys and implications for lithium storage. Acta Materialia, 2003, 51, 1103-1113.	3.8	440
148	Microscale Measurements of the Electrical Conductivity of Doped LiFePO[sub 4]. Electrochemical and Solid-State Letters, 2003, 6, A278.	2.2	200
149	Metal Oxide Composites for Lithium-Ion Battery Anodes Synthesized by the Partial Reduction Process. Journal of the Electrochemical Society, 2002, 149, A1237.	1.3	21
150	Special Issue Ceramics Integration. Liquid-Phase Epitaxial Growth of BaTiO3 Doped(Na0.5Bi0.5)TiO3 Single Crystals on a SrTiO3 Single Crystal Substrate Journal of the Ceramic Society of Japan, 2002, 110, 347-352.	1.3	1
151	Electronically conductive phospho-olivines as lithium storage electrodes. Nature Materials, 2002, 1, 123-128.	13.3	2,684
152	Electrochemically Induced Cation Disorder and Phase Transformations in Lithium Intercalation Oxides. Chemistry of Materials, 2001, 13, 53-63.	3.2	74
153	Relaxor single crystals in the (Bi1/2Na1/2)1â^'xBaxZryTi1â^'yO3 system exhibiting high electrostrictive strain. Journal of Applied Physics, 2001, 90, 5287-5295.	1.1	71
154	Pressure-Induced Pyrochlore-Perovskite Phase Transformation in PLZST Ceramics. , 2001, 6, 7-12.		14
155	Fabrication of functionally graded reaction infiltrated SiC–Si composite by three-dimensional printing (3DP™) process. Materials Science & Engineering A: Structural Materials: Properties, Microstructure and Processing, 2001, 298, 110-119.	2.6	107
156	Magnetic characterization of λ-MnO2 and Li2Mn2O4 prepared by electrochemical cycling of LiMn2O4. Journal of Applied Physics, 2000, 87, 7382-7388.	1.1	40
157	Generalized rheology of active materials. Journal of Applied Physics, 2000, 88, 6902-6909.	1.1	15
158	Spin-glass behavior in LiMn2O4 spinel. Applied Physics Letters, 1999, 74, 2504-2506.	1.5	53
159	Equilibrium-thickness Amorphous Films on {} surfaces of Bi2O3-doped ZnO. Journal of the European Ceramic Society, 1999, 19, 697-701.	2.8	42
160	Electron microscopic characterization of electrochemically cycled LiCoO2 and Li(Al,Co)O2 battery cathodes. Journal of Power Sources, 1999, 81-82, 594-598.	4.0	67
161	Origin of Solid‣tate Activated Sintering in Bi <sub>2</sub> O <sub>3</sub> â€Doped ZnO. Journal of the American Ceramic Society, 1999, 82, 916-920.	1.9	145
162	Effect of Initial Microstructure on Final Intergranular Phase Distribution in Liquidâ€Phaseâ€Sintered Ceramics. Journal of the American Ceramic Society, 1999, 82, 183-189.	1.9	24

#	Article	IF	CITATIONS
163	Lead-free high-strain single-crystal piezoelectrics in the alkaline–bismuth–titanate perovskite family. Applied Physics Letters, 1998, 73, 3683-3685.	1.5	381
164	Thermodynamic Stability of Intergranular Amorphous Films in Bismuthâ€Đoped Zinc Oxide. Journal of the American Ceramic Society, 1998, 81, 89-96.	1.9	122
165	Liquid-exchange processing and properties of SiC–Al composites. Journal of Materials Research, 1997, 12, 1785-1789.	1.2	4
166	Introduction and Overview: Physical Properties of Nanostructured Materials. , 1997, 1, 205-209.		152
167	Model Experiment on Thermodynamic Stability of Retained Intergranular Amorphous Films. Journal of the American Ceramic Society, 1997, 80, 1893-1896.	1.9	30
168	Microstructure development in furfuryl resin-derived microporous glassy carbons. Journal of Materials Research, 1996, 11, 2338-2345.	1.2	18
169	Equilibrium Configuration of Bi-Doped ZnO Grain Boundaries: Intergranular Amorphous Films. Materials Research Society Symposia Proceedings, 1996, 466, 209.	0.1	1
170	Comparisons of Hamaker Constants for Ceramic Systems with Intervening Vacuum or Water: From Force Laws and Physical Properties. Journal of Colloid and Interface Science, 1996, 179, 460-469.	5.0	250
171	Solute Segregation and Grain-Boundary Impedance in High-Purity Stabilized Zirconia. Journal of the American Ceramic Society, 1996, 79, 1169-1180.	1.9	405
172	Reactive-infiltration processing of SiC-metal and SiC-intermetallic composites. Journal of Materials Research, 1996, 11, 2346-2357.	1.2	12
173	Reaction-infiltrated, net-shape SiC composites. Materials Science & Engineering A: Structural Materials: Properties, Microstructure and Processing, 1995, 195, 131-143.	2.6	88
174	Nature of Cation Vacancies Formed to Compensate Donors during Oxidation of Barium Titanate. Journal of the American Ceramic Society, 1995, 78, 909-914.	1.9	38
175	Measurements of Excess Enthalpy in Ultrafine-Grained Titanium Dioxide. Journal of the American Ceramic Society, 1995, 78, 2045-2055.	1.9	57
176	Bi segregation at ZnO grain boundaries in equilibrium with Bi2O3ZnO liquid. Solid State Ionics, 1995, 75, 79-88.	1.3	36
177	Size-dependent solute segregation and total solubility in ultrafine polycrystals: Ca in TiO2. Acta Metallurgica Et Materialia, 1995, 43, 319-328.	1.9	94
178	Thin Glass Film between Ultrafine Conductor Particles in Thick-Film Resistors. Journal of the American Ceramic Society, 1994, 77, 1143-1152.	1.9	136
179	Space Charge Segregation at Grain Boundaries in Titanium Dioxide: I, Relationship between Lattice Defect Chemistry and Space Charge Potential. Journal of the American Ceramic Society, 1993, 76, 2437-2446.	1.9	131
180	Space Charge Segregation at Grain Boundaries in Titanium Dioxide: II, Model Experiments. Journal of the American Ceramic Society, 1993, 76, 2447-2459.	1.9	135

#	Article	IF	CITATIONS
181	Excess Thermodynamic Properties of Nanophase Titanium Dioxide Prepared by Chemical and Physical Methods. Materials Research Society Symposia Proceedings, 1992, 286, 15.	0.1	3
182	Comment on "Interfacial Segregation in Perovskites: I-IV". Journal of the American Ceramic Society, 1992, 75, 2017-2019.	1.9	19
183	Reaction-formed silicon carbide. Materials Science & Engineering A: Structural Materials: Properties, Microstructure and Processing, 1991, 144, 63-74.	2.6	128
184	Grain-Boundary Migration in Nonstoichiometric Solid Solutions of Magnesium Aluminate Spinel: II, Effects of Grain-Boundary Nonstoichiometry. Journal of the American Ceramic Society, 1990, 73, 1153-1158.	1.9	84
185	Liquid-Phase Reaction-Bonding of Silicon Carbide Using Alloyed Silicon-Molybdenum Melts. Journal of the American Ceramic Society, 1990, 73, 1193-1200.	1.9	124
186	Grain-Boundary Chemistry of Barium Titanate and Strontium Titanate: I, High-Temperature Equilibrium Space Charge. Journal of the American Ceramic Society, 1990, 73, 3278-3285.	1.9	325
187	Grain-Boundary Chemistry of Barium Titanate and Strontium Titanate: II, Origin of Electrical Barriers in Positive-Temperature-Coefficient Thermistors. Journal of the American Ceramic Society, 1990, 73, 3286-3291.	1.9	120
188	Nonequiiibrium Surface Segregation in Aluminum-Doped TiO2 under an Oxidizing Potential: Effects on Redox Color-Boundary Migration. Journal of the American Ceramic Society, 1990, 73, 1633-1640.	1.9	28
189	Grain-Boundary Migration in Nonstoichiometric Solid Solutions of Magnesium Aluminate Spinel: I, Grain Growth Studies. Journal of the American Ceramic Society, 1989, 72, 271-277.	1.9	93
190	Sequential Precipitation of MgAl2O4 on Mg1-x CaxAl2O4 in Hot-Pressed MgO Single Crystals. Journal of the American Ceramic Society, 1988, 71, 197-200.	1.9	1
191	Dense and Refractory Silicon Carbide by New Reaction Bonding Process. Materials and Processing Report, 1988, 2, 4-5.	0.0	0
192	Spin-On thin films of YBa <sub>2</sub> Cu <sub>3</sub> O <sub>7-y</sub> and La <sub>2â^²x</sub> Sr <sub>x</sub> CuO <sub>4-y</sub> from Citrate-Polymer Precursors. Materials Research Society Symposia Proceedings, 1987, 99, 307.	0.1	11
193	Grain Boundary Segregation and Thermal History Effects on Properties of La1.85Sr0.15CuO4-y Superconductors. Materials Research Society Symposia Proceedings, 1987, 99, 821.	0.1	1
194	Spinodal Decomposition in a K2O-Al2O3-CaO-SiO2 Glass. Journal of the American Ceramic Society, 1983, 66, c171-c172.	1.9	17
195	Methods—A Potential–Dependent Thiele Modulus to Quantify the Effectiveness of Porous Electrocatalysts. Journal of the Electrochemical Society, 0, , .	1.3	3